Acta of Bioengineering and Biomechanics
Vol. 19, No. 4, 2017

Original paper
DOI:10.5277/ABB-00911-2017-03

Integration of reliability analysis into mini-plate fixation strategy used in human mandible fractures: Convalescence and healing periods

GHIAS KHARMANDA[1], ABDALLAH SHOKRY[2]*, MOHAMED Y. KHARMA[3]

[1] Department of Biomedical Engineering, Lund University, Sweden.
[2] Department of Mechanical Engineering, Fayoum University, Egypt.
[3] Department oral maxillofacial surgery, Al-Farabi College for Dentistry, Saudi Arabia.

Purpose: The objective was to assess the reliability level of mini-plate fixation used in fracture mandibles in order to evaluate the structure stability in both convalescence and healing periods.

Methods: In the convalescence period, the failure scenario is measured by the relative displacement between two fracture surfaces which should not exceed an acceptable value in order to obtain a good stability for rapid bone healing and to limit any trauma. However, in the healing period, it is the objective to obtain an acceptable rigidity. Hereby, the failure scenario is measured by the von Mises stresses being as indicator of mandible fractures.

Results: During the surgery operation, some muscles can be cut or harmed and cannot operate at its maximum capability. Thus, there is a strong motivation to introduce the loading uncertainties in order to obtain reliable designs. A 3-dimensional finite element model was developed in order to study the negative effect caused by stabilization of the fracture. The different results were obtained when considering a clinical case of a 35-year-old male patient. The results show the importance of fixation of symphysis fracture by two I-plates with four holes. The structural reliability level was estimated when considering a single failure mode and multiple failure modes.

Conclusions: The integration of reliability concepts into mini-plate fixation strategy is considered a novel aspect. The reliability evaluation seams to be a reasonable asset in both convalescence and healing periods.

Key words: *structural optimization, structural reliability, mandible fractures, mini-plate fixation*

1. Introduction

Fracture of the mandible is one of the most common bone injuries, because of its prominence, mobility and exposed position within the facial skeleton. They are caused mostly because of motor vehicle crashes, falls, violence, and sports. There are several types of mandibular fractures depending on their location. The most common area of fracture is at the condyle (36%), body (21%), angle (20%) and symphysis (14%). The choice of imaging technique (CT, panoramic radiography...) for mandibular fracture indication essentially depends on its location [19], [25]. The present paper concentrates on a symphysis mandible fracture type. In previous investigation related to symphysis mandible fracture studies [17], muscle forces have been ignored and only the bite force was applied, and the mandible was fixed at its ends. For this loading case, Korkmaz [17] investigated several mini-plate systems and provided recommendations regarding mini-plate location, orientation, and

* Corresponding author: Abdallah Shokry, Fayoum University, 63514 Fayoum, Egypt. Tel. 002 01094999199, e-mail: abdallah.shokry@fayoum.edu.eg

Received: May 15th, 2017
Accepted for publication: September 13th, 2017

selection of type. Recently, several muscle forces have been considered (masseter, temporalis, lateral and medial pterygoïd forces). In order to show the role of these forces, an efficient structural optimization strategy was integrated [15]. Hereby, the topology optimization process was considered a conceptual design stage to sketch the layout "or input" to shape optimization. After that both shape and sizing optimization were considered a detailed design stage. This strategy provided a suitable fixation with acceptable rigidity which allows the tow fragment fracture to be kept in good stability for rapid bone healing and limit any trauma to adjacent nerves. And the resulting topology also takes into account the ideal line for osteosynthesis presented by Champy et al. [1]. The principle of osteosynthesis, according to Champy, is to reestablish mechanical qualities of the mandible. Mini-plate osteosynthesis is an internal procedure for repairing fractures of the mandible, maxilla, by using titanium plates or mini-plates and screws to stabilize the bone fragments in proper alignment. The purpose of all therapies of fractures is the restoration of the original form and function with immobilization being one of the most important factors. The fracture during the healing process is extremely susceptible to mechanical influences [16]. Mobility the fracture site is one of the main causes of healing disturbances [24].

In reliability context, in the classical deterministic designs, a safe performance cannot be completely guaranteed, due to the uncertainty of different bone properties, geometry and loading. In the present study, different external forces are considered as uncertain parameters in both convalescence (after surgical operation) and healing periods. The first of these periods represents the gradual recovery of health and strength after the surgical operation, in which a frictional contact between fracture surfaces is considered, while the healing period is starts when a full contact surface is created between both fracture surfaces. During the convalescence and healing periods, several critical failure modes can occur. Evidently, failure due to, e.g., screw loosening can be included, but it is out of the scope of the present investigation. However, in this study it was considered that the relative displacement between fracture surfaces yield in the plates and bone and the bone remodeling are critical failure modes. Then, a reliability algorithm was developed in order to assess the reliability level for single and multiple failure modes. Finally an application on a clinical case of a male patient of 35 years of age was carried out to show the applicability of the reliability strategy proposed.

2. Material and methods

2.1. Problem description (clinical case study)

Figure 1 presents an orthopantomogram of a male patient at the age of 35 years. The surgical operation was carried out at Aleppo University Hospital [15]. All the basic principles of internal fixation were followed. In mandibular fractures, the plates were placed along the ideal lines of osteosynthesis as described by Champy et al. [1]. At least two screws were placed on each segment in all the cases. There were no specific complications related to his treatment and the healing period lastet for about three months.

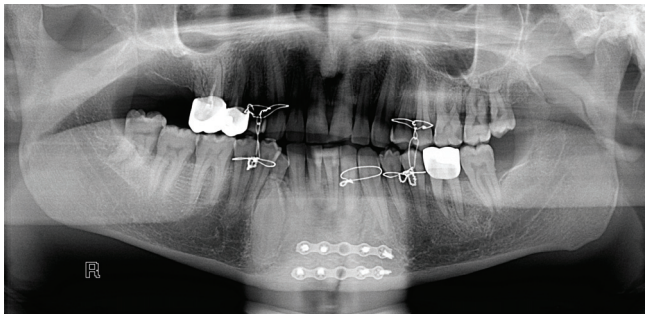

Fig. 1. Orthopantomogram of a male patient of age 35 years [15]

2.2. Mechanical properties

The mechanical properties of bone depend on its composition and structure. It is well-known that the bone material structure is complex and shows an anisotropic mechanical response. The mandibular bone properties are orthotropic materials. In order to perform a reliability analysis or/and an optimization process, a new formulation relating the yield stress and the Young's modulus for orthotropic bone properties should be established and integrated to a reliability or/and an optimization loop(s). In this case, several experimental tests were needed to approximate the required formulations. However, there are not enough experimental results of the mandibular bone reported. Therefore, a simplified bone model is here considered to be isotropic, homogeneous, and linearly elastic [7]. Its elastic behavior is characterized by two material constants (Young's modulus E and Poisson's ratio ν). The most representative compositional variable is the ash density ρ_α with the following correlation [12]:

$$E = 10500\rho_{\alpha}^{2.57\pm0.04} \quad (1)$$

$$\sigma_C = 117\rho_{\alpha}^{1.93\pm0.04} \quad (2)$$

where σ_C is the yield stress in compression. These expressions explain over 96% of the statistical variations in the mechanical behaviour of combined vertebral and femoral data over the range of ash density (ρ_α = (0.03÷1.22 g/cm^3)). In the literature, several works correlate mechanical properties of bone materials with its composition [5]. Recently, an accurate formulation for yield stress against elasticity modulus relationship has been proposed to directly correlate the mechanical properties of bone materials [13]. The relationship is written as follows:

$$\sigma_C = 129.5\left(\frac{E}{11142}\right)^{0.94}. \quad (3)$$

Introducing the tension/compression ratio $R_{T/C}$, the yield stress in tension is obtained as:

$$\sigma_T = R_{T/C}.\sigma_C. \quad (4)$$

Different values have been used for the ratio $R_{T/C}$, ranging from 0.5 to 0.7 for cortical bone and from 0.7 to 1 for cancellous bone [5]. It was concluded that the yield stress in tension is always less than the yield stress in compression [11]. Based on this observation, the yield stress in tension was used as a maximum allowable stress value in the mandible. A model with cortical and cancellous bone was considered. The mechanical properties for the cortical tissue are: E = 15750 MPa and ν = 0.325 and for cancellous tissue are: E = 300 MPa, ν = 0.30. These values were obtained from a previous study [23]. In addition, the material properties of the used mini-plates and screws were assigned for titanium as 110 GPa for Young modulus and 0.34 for the Poisson ratio [17]. However, to compute the yield stress in tension, Eq. (4) leads to $\sigma_T \in$ [90–125] MPa for the cortical bone when considering the ratio $R_{T/C}$ = [0.5–0.7] and $\sigma_T \in$ [3–4] MPa for the cancellous bone when considering the ratio $R_{T/C}$ = [0.7–1] [6]. The properties of materials used in this work are presented in Table 1.

Table 1. Material properties used in the studied finite element model

Material	Young's modulus [MPa]	Poisson's ratio	Yield stress in compression [MPa]	Yield stress in tension [MPa]
Titanium	110000	0.34	860	860
Cortical Bone	15750	0.325	180	90–125
Cancellous Bone	300	0.3	4.0	3–4

2.3. Boundary conditions

In realistic studies, several loading types can be considered during the reliability analysis such as biting, chewing and mastication processes. In this case, a complicated problem with different kinds of applied forces (bite and different oblique forces) should be considered [26]–[28]. That leads to a great number of optimization variables which are not accessible in the version of ANSYS software used in this study, with only 20 input parameters are available. Therefore, a bite force case is considered in this study where several muscle forces are accounted. In previous study of Korkmaz [17], a single applied bite force has been considered. However, in order to obtain much more realistic simulation models, the positive role of muscle forces has been demonstrated [15]. During the bite process, the digastric muscles are not very active and, therefore, not included in analysis [22]. Figure 2 depicts an illustration of the twelve muscle forces (six on each side) applied to the mandible [21]. In order to study the effect of the temporal-mandibular joint, a dynamic study is required to simulate the different movements. In literature, several simplifications can be found in experimental and numerical studies in order to apply a static analysis on the temporal-mandibular joint [18]. In the present work, a static study can be carried out

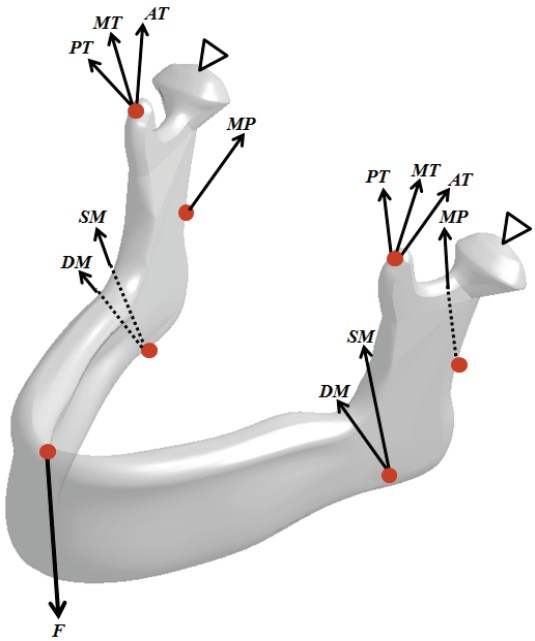

Fig. 2. Boundary conditions of a healthy mandible

by separating the mandible (lower part) from the whole system. Therefore, this mandible is fixed at its extremities, as shown in Fig. 2, which is in accordance with the assumptions of Korkmaz [17] and Kharmanda et al. [15]. The values applied for each force are presented in Table 2.

Table 2. Muscle forces [21]

Muscle Forces	F_x [N]	F_y [N]	F_z [N]
Superficial Masseter (SM)	18.2	303.3	12.1
Deep Masseter (DM)	7.8	128.3	15.6
Anterior Temporalis (AT)	–18.4	104.8	–43.8
Medial Temporalis (MT)	–6.5	36.3	–53.1
Posterior Temporalis (PT)	–3.4	6.8	–37
Medial Pterygoid (MP)	187.4	325.1	–76.5

2.4. Reliability analysis

In structural reliability theory, many effective techniques have been developed during the last 40 years to estimate the reliability, namely FORM (First Order Reliability Methods), SORM (Second Order Reliability Method) and simulation techniques [4]. The reliability problem can be performed for a single failure mode and for multiple failure modes.

2.4.1. Single Failure Mode (S.F.M.)

The transformation of the random variables y in the standard normalized space is denoted u, and calculated by: $u = T(y)$ where $T(y)$ is the probabilistic transformation function. The mean value m_i of the random variable y_i is considered the origin of the normalized space (see Fig. 3). For a given failure scenario $H(u) = 0$, the reliability index β is evaluated by solving a constrained minimization problem:

$$\beta = \min d(u) \quad \text{subject to:} \quad H(u) = 0 \tag{5}$$

with

$$d = \sqrt{\sum u_i^2} \tag{6}$$

where u is the variable vector in the normalized space, measured from the origin (Fig. 3).

The solution to problem (5) defines the Most Probable failure Point (MPP), (Fig. 3b). The resulting minimum distance between the limit state function $H(u)$ and the origin, is called the reliability index β [10]. The reliability index that corresponds to the probability of failure, is numerically computed as follows

$$P_f \approx \Phi(-\beta_t) \tag{7}$$

where $\Phi(.)$ is the standard Gaussian cumulated function given as follows:

$$\Phi(Z) = \frac{1}{\sqrt{2\pi}} \int_{-\infty}^{Z} e^{-\frac{z^2}{2}} dz, \tag{8}$$

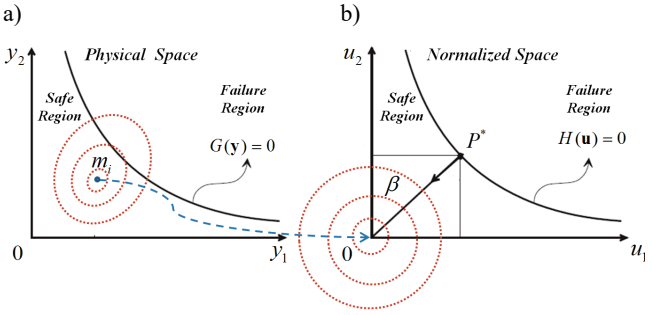

Fig. 3. Physical and normalized spaces for single failure mode

For practical structural engineering studies, equation (7) gives sufficiently accurate estimation of the failure probability [14]. Fig. 4 shows a flowchart of the MPP algorithm. It consists of two nested optimization loops. The objective of the first one is to find a failure point belonging to the limit state ($G(y) = 0$) in the physical space, (Fig. 3a). The second loop tests the reliability levels for several failure points in order to find the MPP which belongs to the limit state ($H(u) = 0$) in the normalized space. The MPP state is found at the minimum distance to the origin of the normalized space. For the convalescence period, the failure scenario takes place when the relative displacement between fracture surfaces exceeds the allowable (or target) value. However, for the healing period, the failure scenario occurs when one of the given yield stresses is exceeded (equation (4)).

2.4.2. Multiple Failure Modes (M.F.M.)

When multiple conflicting criteria are involved in evaluating a complex design system consisting of several constraint functions have to be used. This way problem (5) can be written as follows:

$$\beta = \min d(u) \quad \text{subject to}: \quad H(u) = 0 \tag{9}$$

where $H(u) = 0$ is the vector of limit state functions (equality constraints). For example, Fig. 5 shows the physical and the normalized spaces for double failure modes (limit states). The global optimum solution in the normalized space is given by the minimum distance between the intersection point P^* and the origin. The developed reliability algorithm shown in Fig. 4

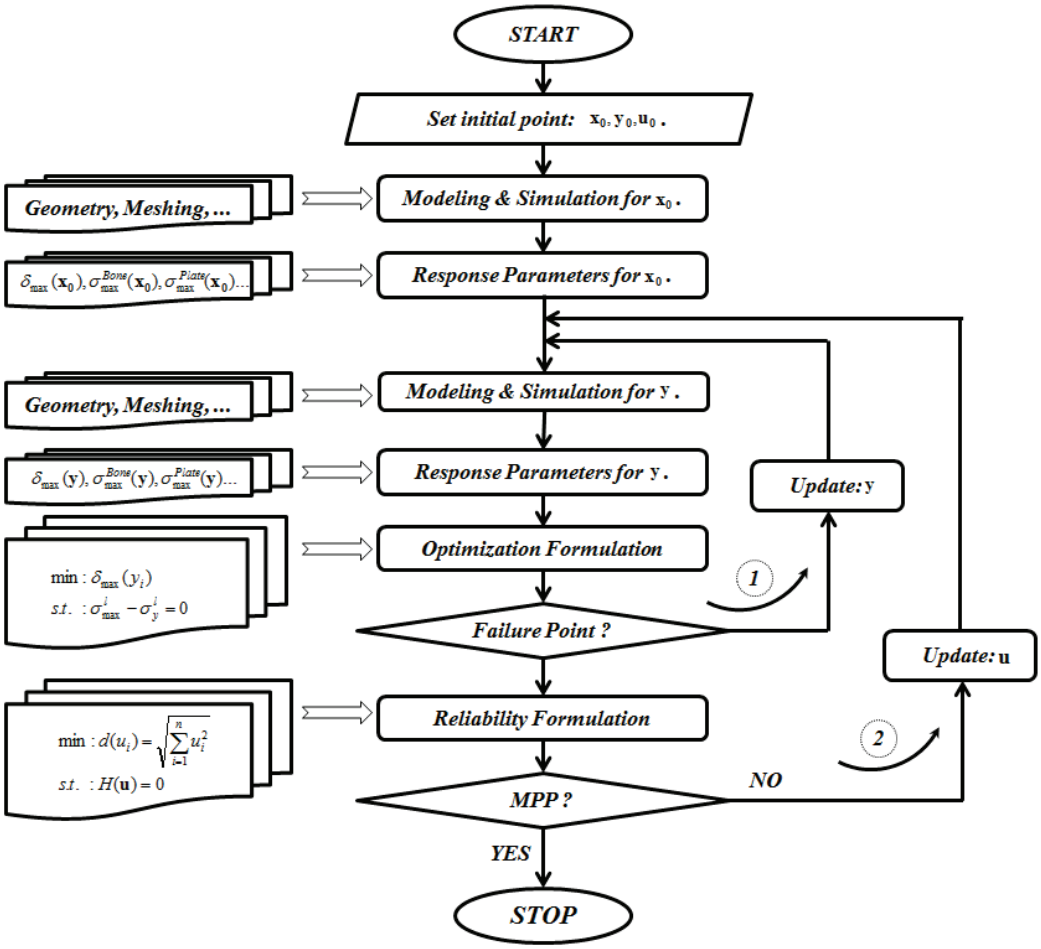

Fig. 4. Flowchart of MPP algorithm

provides a global optimum within a reasonable computing time.

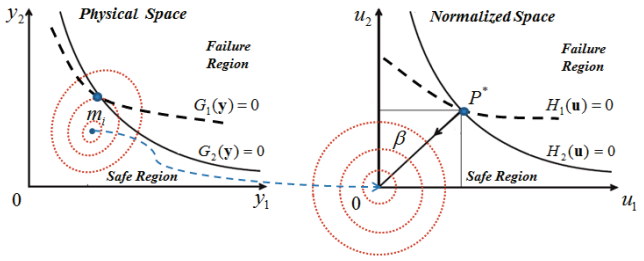

Fig. 5. Physical and normalized spaces for multiple failure modes

3. Results

3.1. Studied model

In the studied model, due to the limited influence of the teeth on the mechanical response of the mandible, these teeth were ignored and removed in order to simplify the modeling. The mono-cortical screws were also modeled as simple cylinders of a length appropriate for penetration. According to the clinical observations of Cox et al. [3], the upper limit of relative movement of the blocks of a broken mandible in the fracture section under a bite forces should not exceed 150 μm, what is assumed as the limit value of sliding. According to Gross and Abel [9], the von Mises stress values are considered a fracture indicator. This way the maximum values should not exceed the yield stress values in tension σ_T (Eq. (4)). The loading case is that the mandible is subjected to a bite force and all muscle forces are active and fixed at its extremities (Fig. 6). The bite force is applied in regions *A* and *B*. The applied muscle forces: M^{Right} and M^{Left} denote the sum of the masseter muscles (regions *C* and *D*). T^{Right} and T^{Left} denote Temporalis muscles (regions *E* and *F*). P^{Right} and P^{Left} denote the sum of medial and lateral pterygoid muscles (regions *G* and *H*). The fixation is considered in regions *I* and *J*. According to the experimental results of Kumar et al. [20], the maximum bite force value (F_b) was assumed 44 N after the surgical operation and 208 N in the healing

period. The mean values of all forces are presented in Tables 3 and 5 for convalescence and healing periods, respectively. Because of lack of experimental data, the random variables are presumed to be normally distributed and the standard-deviations are assumed proportional to the mean values [14].

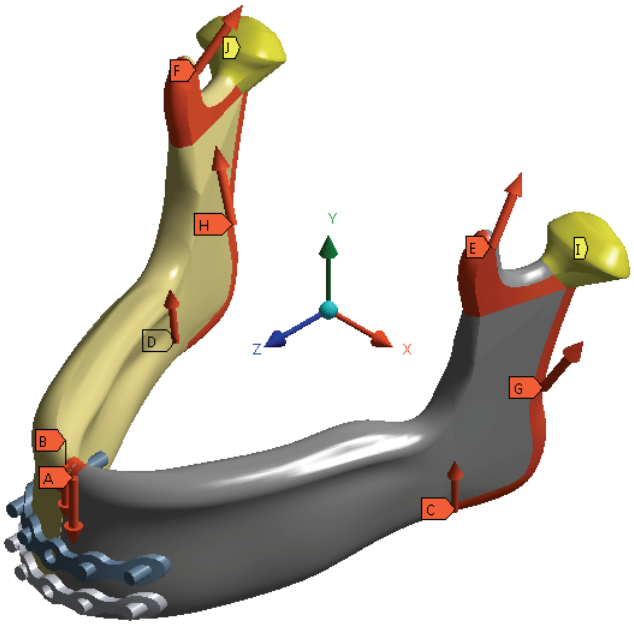

Fig. 6. Boundary conditions of the fractured mandible

In the present study the bite force and the most effective muscle force components are considered as random variables. The random variable vector then contains 20 components: 2 for the bite and 18 for the muscle forces. In order to get acceptable levels of rigidity and a limited displacement at the fracture line, double I mini-plates were fixed to the bone with eight screws as shown in Fig. 6.

3.2. Reliability assessment of convalescence period

In covalescence period the patient is advised to bite soft foods in order to apply small values of bite forces. The muscle forces are automatically prepared to balance the mandible system. Hereby, it is important to introduce the uncertainty of different forces in order to guarantee a safe performance, taking into account the osseointegration process and the overloading possibility. In Table 3, the mean value of the bite force is: F_b = 44 (N) and the muscle forces are proportionally calculated relative to the maximum unfractured mandible capability [21]. A direct simulation shows that the maximum total displacement is 0.1 mm and the maximum von Mises stress occurred at the lower mini-plate was equal to 72.22 MPa (Fig. 7).

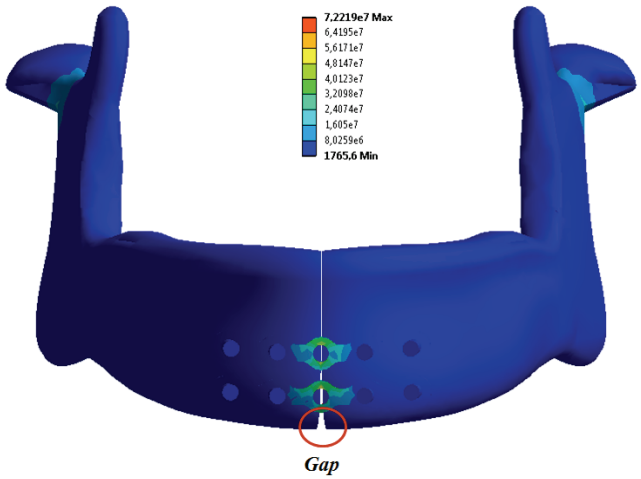

Fig. 7. Von Mises stress distribution for the convalescence period

Table 3. Resulting parameter values for convalescence period

Parameters		Means	Design Interval	MPP
F^{Bite} [N]	F_y^{Right}	–22	$-41.8 \le F_y^{\text{Right}} \le -2.2$	–36.82
	F_y^{Left}	–22	$-41.8 \le F_y^{\text{Left}} \le -2.2$	–33.89
M^{Right} [N]	M_x^{Right}	5.46	$0.55 \le M_x^{\text{Right}} \le 10.37$	7.31
	M_y^{Right}	90.64	$9.06 \le M_y^{\text{Right}} \le 172.21$	15.91
	M_z^{Right}	5.82	$0.58 \le M_z^{\text{Right}} \le 11.05$	3.63
M^{Left} [N]	M_x^{Left}	–5.46	$-0.55 \le M_x^{\text{Left}} \le -10.37$	–8.38
	M_y^{Left}	90.64	$9.06 \le M_y^{\text{Left}} \le 172.21$	54.69
	M_z^{Left}	5.82	$0.58 \le M_z^{\text{Left}} \le 11.05$	5.10
T^{Right} [N]	T_x^{Right}	–5.94	$-0.59 \le T_x^{\text{Right}} \le -11.29$	–9.51
	T_y^{Right}	31.06	$3.11 \le T_y^{\text{Right}} \le 59.01$	8.25
	T_z^{Right}	–28.12	$-2.81 \le T_z^{\text{Right}} \le -53.43$	–48.48
T^{Left} [N]	T_x^{Left}	5.94	$0.59 \le T_x^{\text{Left}} \le 11.29$	2.02
	T_y^{Left}	31.06	$3.11 \le T_y^{\text{Left}} \le 59.01$	5.02
	T_z^{Left}	–28.12	$-2.81 \le T_z^{\text{Left}} \le -53.43$	–50.10
P^{Right} [N]	P_x^{Right}	39.35	$3.94 \le P_x^{\text{Right}} \le 74.77$	56.96
	P_y^{Right}	68.27	$6.83 \le P_y^{\text{Right}} \le 129.71$	12.93
	P_z^{Right}	–16.07	$-1.61 \le P_z^{\text{Right}} \le -30.52$	–29.29
P^{Left} [N]	P_x^{Left}	–39.35	$-3.94 \le P_x^{\text{Left}} \le -74.77$	–55.18
	P_y^{Left}	68.27	$6.83 \le P_y^{\text{Left}} \le 129.71$	36.19
	P_z^{Left}	–16.07	$-1.61 \le P_z^{\text{Left}} \le -30.52$	–26.66

Hereby, the maximum initial relative displacement between two fracture surfaces $\delta_{\max}$ amounts to 121 μm. The resulting maximum stress values at the mean point are presented in Table 4. Based on Eq. (5), the reliability index of the structure was estimated. When

considering small tolerances for force variability, the different constraints are not being violated. Here, the variability intervals are increased to ±90% of mean values of the muscle forces. The relative displacement constraint is the first one to be violated. Referring to Table 4, it can be concluded that the most critical constraint (limit state) is the maximum relative displacement at the fracture line $H(u_i) = \delta_{\max} - \delta_w = 0$ considering that its acceptable limit to be $\delta_w = 150$ μm [3]. The reliability index considering the force variability of the studied structure equals to $\beta = 3.08$, which corresponds to probability of failure $P_f \approx 1 \times 10^{-3}$ applying Eq. (7).

3.3. Reliability assessment of healing period

During the healing period, several failure scenarios can occur if certain values of stresses or strains exceeded the target limits. The maximum values of von Mises stresses in different tissues are considered the fracture indicators and the maximum values of the principal strains in different tissues are considered the bone remodeling indicators. Thus, these indicators should be included as constraints in the reliability analysis procedures. In addition, the healing period takes into consideration the time taken for the bite forces to return to a normal functional range. According to Kumar et al. [20], the highest bite force generated by a control group is 208 N in the anterior region of the mandible.

Similar findings were reported by Ellis and Throckmorton [6]. A direct simulation shows that the maximum total displacement is 0.3 mm and the maximum von Mises stress occurred in cortical bone of the right part is 71.45 MPa (Fig. 8).

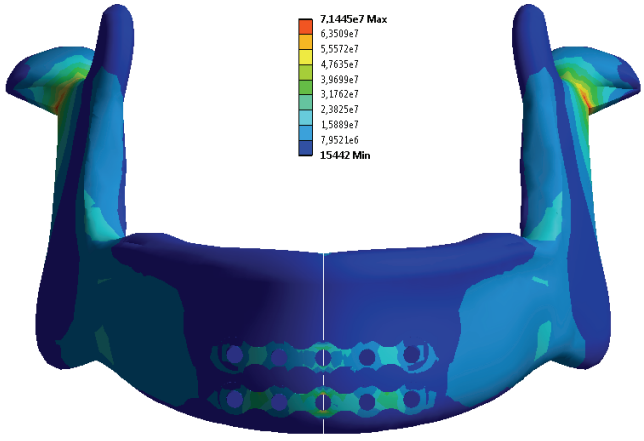

Fig. 8. Von Mises stress distribution for the healing period

Table 4. Resulting response values for convalescence period

Parameters	Means	Design Interval	MPP
$\sigma_{\max}^{\text{Upper}}$ [MPa]	54.07	$1.48 \le \sigma_{\max}^{\text{Upper}} \le 136.12$	99.11
$\sigma_{\max}^{\text{Lower}}$ [MPa]	72.22	$1.69 \le \sigma_{\max}^{\text{Lower}} \le 176.38$	125.00
$\sigma_{\max}^{\text{CorRight}}$ [MPa]	19.03	$6.58 \le \sigma_{\max}^{\text{CorRight}} \le 72.10$	40.52
$\sigma_{\max}^{\text{CanRight}}$ [MPa]	0.07	$0.01 \le \sigma_{\max}^{\text{CanRight}} \le 0.24$	0.12
$\sigma_{\max}^{\text{CorLeft}}$ [MPa]	18.42	$3.85 \le \sigma_{\max}^{\text{CorLeft}} \le 68.30$	37.05
$\sigma_{\max}^{\text{CanLeft}}$ [MPa]	0.11	$0.02 \le \sigma_{\max}^{\text{CanLeft}} \le 0.38$	0.20
$\delta_{\max}$ [μm]	121	$0 \le \delta_{z_{\max}} \le 150$	149.1
β	–	$\beta \ge 3.08$	3.08
P_f		$P_f \le 1.04 \times 10^{-3}$	1.04×10^{-3}

When considering small tolerance variability intervals (±10% of the muscle force mean values), three constraints are violated. The stress constraints of the right and left mandible parts ($\sigma_{\max}^{\text{CorRight}} = 372.44 > \sigma_y^{\text{Cor}} = 90$ MPa and $\sigma_{\max}^{\text{CorLeft}} = 124.55 > \sigma_y^{\text{Cor}} = 90$ MPa [15], see Tables 1 and 6) and the strain constraint of the right cortical part exceeded their limitations ($\varepsilon_{\max}^{\text{CorRight}} = 0.028 > \varepsilon_w^{\text{Cor}} = 0.02$ [8]). Thus, it is concluded that the most critical constraints may occur at the maximum values of von Mises stress in cortical bone of the right part and/or the left one and may also at the maximum value of the principal strain in the right cortical part (Table 6). This way, two cases (a single failure mode and a Multiple Failure modes) can be studied.

3.3.1. Single failure mode (S.F.M.)

According to the results, a single failure mode can occur at the cortical bone of the right part or the left one before the violation of the maximum principal strain constraint. Based on Eq. (5), the reliability index of the structure is first estimated for the limit state $H(u_i) = \sigma_{\max}^{\text{Right}} - \sigma_y^{\text{Right}} = 0$. The resulting reliability index considering the force variability of the studied structure equals to $\beta = 3.12$ that corresponds to the probability of failure $P_f \approx 9.04 \times 10^{-4}$. In addition, when considering the limit state function at the left part $H(u_i) = \sigma_{\max}^{\text{Left}} - \sigma_y^{\text{Left}} = 0$, the resulting reliability index equals to: $\beta = 4.85$, which corresponds to the probability of failure $P_f \approx 6.17 \times 10^{-7}$. However, when considering the limit state function at the maximum principal strain function $H(u_i) = \varepsilon_{\max}^{\text{CorRight}} - \varepsilon_w^{\text{Cor}} = 0$, no convergence has been registered.

Table 5. Resulting parameter values for healing period

Parameters		Means	Design Interval	MPP		
				S.F.M.		M.F.M.
				Right	Left	Both
F^{Bite} [N]	F_y^{Right}	–104	$-200 \le F_y^{\text{Right}} \le -50$	–119.75	–68.85	–74.08
	F_y^{Left}	–104	$-200 \le F_y^{\text{Left}} \le -50$	–98.47	–79.43	–67.06
M^{Right} [N]	M_x^{Right}	26	$23.4 \le M_x^{\text{Right}} \le 28.6$	28.50	24.66	26.96
	M_y^{Right}	431.6	$388.44 \le M_y^{\text{Right}} \le 474.76$	442.04	453.11	466.68
	M_z^{Right}	27.7	$24.93 \le M_z^{\text{Right}} \le 30.47$	28.14	27.93	29.73
M^{Left} [N]	M_x^{Left}	–26	$-28.6 \le M_x^{\text{Left}} \le -23.4$	–24.15	–26.36	–26.73
	M_y^{Left}	431.6	$388.44 \le M_y^{\text{Left}} \le 474.76$	397.55	464.17	441.25
	M_z^{Left}	27.7	$24.93 \le M_z^{\text{Left}} \le 30.47$	25.67	29.97	27.18
T^{Right} [N]	T_x^{Right}	–28.3	$-31.13 \le T_x^{\text{Right}} \le -25.47$	–29.81	–26.02	–30.14
	T_y^{Right}	147.9	$133.11 \le T_y^{\text{Right}} \le 162.69$	142.33	155.15	148.00
	T_z^{Right}	–133.9	$-147.29 \le T_z^{\text{Right}} \le -120.51$	–142.18	–147.21	–121.45
T^{Left} [N]	T_x^{Left}	28.3	$25.47 \le T_x^{\text{Left}} \le 31.13$	29.53	30.09	26.00
	T_y^{Left}	147.9	$133.11 \le T_y^{\text{Left}} \le 162.69$	146.07	144.56	153.59
	T_z^{Right}	–133.9	$-147.29 \le T_z^{\text{Right}} \le -120.51$	–139.25	–144.22	–134.55
P^{Right} [N]	P_x^{Right}	187.4	$168.66 \le P_x^{\text{Right}} \le 206.14$	177.58	174.80	188.24
	P_y^{Right}	325.1	$292.59 \le P_y^{\text{Right}} \le 357.61$	301.11	339.43	348.46
	P_z^{Right}	–76.5	$-84.15 \le P_z^{\text{Right}} \le -68.85$	–83.90	–74.28	–71.36
P^{Left} [N]	P_x^{Left}	–187.4	$-206.14 \le P_x^{\text{Left}} \le -168.66$	–202.97	–194.49	–197.71
	P_y^{Left}	325.1	$292.59 \le P_y^{\text{Left}} \le 357.61$	349.41	316.88	341.88
	P_z^{Left}	–76.5	$-84.15 \le P_z^{\text{Left}} \le -68.85$	–71.97	–69.18	–76.11

Table 6. Resulting response values for healing period

Parameters	Means	Design Interval	MPP		
			S.F.M.		M.F.M.
			Right	Left	Both
$\sigma_{\max}^{\text{Upper}}$ [MPa]	34.19	$25.17 \le \sigma_{\max}^{\text{Upper}} \le 46.88$	35.26	30.87	32.32
$\sigma_{\max}^{\text{Lower}}$ [MPa]	61.96	$44.04 \le \sigma_{\max}^{\text{Lower}} \le 88.39$	63.99	54.70	56.80
$\sigma_{\max}^{\text{CanRight}}$ [MPa]	1.06	$0.78 \le \sigma_{\max}^{\text{CanRight}} \le 1.52$	1.09	0.93	0.96
$\sigma_{\max}^{\text{CorRight}}$ [MPa]	71.45	$75.60 \le \sigma_{\max}^{\text{CorRight}} \le 372.44$	89.99	86.02	89.86
$\sigma_{\max}^{\text{CanLeft}}$ [MPa]	1.02	$0.91 \le \sigma_{\max}^{\text{CanLeft}} \le 3.58$	1.21	1.15	1.18
$\sigma_{\max}^{\text{CorLeft}}$ [MPa]	69.06	$56.30 \le \sigma_{\max}^{\text{CorLeft}} \le 124.55$	69.35	89.82	89.64
$\varepsilon_{\max}^{\text{CanRight}}$	0.004	$0.003 \le \varepsilon_{\max}^{\text{CanRight}} \le 0.005$	0.004	0.003	0.003
$\varepsilon_{\max}^{\text{CorRight}}$	0.004	$0.003 \le \varepsilon_{\max}^{\text{CorRight}} \le 0.028$	0.007	0.005	0.006
$\varepsilon_{\max}^{\text{CanLeft}}$	0.002	$0.002 \le \varepsilon_{\max}^{\text{CanLeft}} \le 0.013$	0.003	0.003	0.003
$\varepsilon_{\max}^{\text{CorLeft}}$	0.002	$0.002 \le \varepsilon_{\max}^{\text{CorLeft}} \le 0.007$	0.002	0.003	0.004
β	–	$\beta \ge 3.12$	3.12	4.85	5.10
P_f	–	$P_f \le 9.04 \times 10^{-4}$	9.04×10^{-4}	6.17×10^{-7}	1.70×10^{-7}

3.3.2. Multiple failure modes (M.F.M.)

The multiple failure modes can occur at the cortical bone of the right part and the left one before the violation of the maximum principal strain constraint. This way the MPP is assumed to be located at the intersection of several constraint functions (limit states). The only one of failure modes that will occur, is the mandible fracture. Thus, the considered limit states are: $H_1(u_i) = \sigma_{\max}^{\text{CorRight}} - \sigma_y^{\text{Cor}} = 0$ and $H_2(u_i) = \sigma_{\max}^{\text{CorLeft}} - \sigma_y^{\text{Cort}} = 0$.

The resulting system reliability index is then equal to $\beta = 5.10$, which corresponds to a very small probability of failure $P_f \approx 1.70 \times 10^{-7}$.

4. Discussion

The primary goal of fracture management is healing of the fractured bone, resulting in restoration of form and function. Modern traumatology started with the development of osteosynthesis using mini-plates for the treatment of fractures. In the present study, the correct position of mini-plates was confirmed in the symphysis fracture respecting the ideal line for osteosynthesis presented by Champy [1]. Korkmaz [17] has tested several types of mini-plate used in the fractured mandible treatment. An assumption was made that the mandible is made exclusively of cortical bone [17]. This is a very important assumption that could likely result in failure in accurate prediction of failure of the bone. Therefore, double tissues (cortical and cancellous tissues) are considered in this work to improve the failure prediction accuracy. His results led to the importance of fixation of symphysis or parasymphysis fracture by two I-plates with four holes.

Korkmaz [17] applied a bite force without taking the muscle forces into consideration. In previous work of Kharmanda et al. [15], it has been demonstrated that the resulting maximum stress when ignoring the muscle forces, exceeds the yield strength of the bone. Therefore, the integration of different muscle forces leads to reasonable values because the muscle forces play a positive role in the equilibrium. In fact, some muscles can be cut or harmed during the surgery, and it cannot be expected that all muscles will operate at its maximum capability. Therefore, there is a strong need to integrate the uncertainty on the muscle forces. In our study, two essential cases were evaluated (convalescence and healing cases). In convalescence period (after surgical operation), it is considered that there are no osseointegration layers between fracture surfaces. Here, small bite force values can be applied when considering soft foods. During the bite process, a sliding movement may occur between both fracture surfaces. This movement must be limited to avoid any trauma and to support the osseointegration process in order to reduce the healing period. This objective can be attended when considering that the relative displacement between both fracture surfaces must not exceed an acceptable value ($\delta_{\max} \leq 150$ μm). If the fracture-gap width is larger than the allowable value, bone healing will be delayed. So a good reduction of a fracture with small interfragmentary gaps is important for its revascularization and healing which can be achieved by rigid fixation [2].

In the healing period, critical failure takes place when outputs exceed their defined limits, such as the fracture indicator [9] represented by the maximum von Mises stress values of plates and/or bone and also the bone remodeling indicator [8] and the maximum principal strain of cortical tissue. Here, the algorithm provides several solutions for single and multiple failure modes. When considering the single failure mode, the scenario of failure may occur in one of both mandible parts ($\sigma_{\max}^{\text{CorRight}}$ or $\sigma_{\max}^{\text{CorLeft}}$). However, for the multiple failure modes, the scenario of failure may take place in both mandible parts ($\sigma_{\max}^{\text{CorRight}}$ and $\sigma_{\max}^{\text{CorLeft}}$). No failure has been registered when considering the bone remodeling indicator ($\varepsilon_{\max}^{\text{CorRight}}$ or $\varepsilon_{\max}^{\text{CorLeft}}$).

In general, the failure probability of structural studies should be: $P_f \in [10^{-3}–10^{-5}]$, which corresponds to a reliability index interval $\beta \in [3–4.25]$, however in nuclear and spatial ones the failure probability should be very small: $P_f \in [10^{-6}–10^{-8}]$, what corresponds to a reliability index $\beta \in [4.75–5.6]$. The different results of the convalescence period in Table 4 show a single failure mode with a reasonable value of reliability index $\beta = 3.08$, which corresponds to failure probability $P_f \approx 1.04 \times 10^{-3}$. Furthermore, for the healing period, the single failure mode may occur in the right mandible part ($\sigma_{\max}^{\text{CorRight}} \approx \sigma_y^{\text{Cor}}$) or in the left mandible part ($\sigma_{\max}^{\text{CorLeft}} \approx \sigma_y^{\text{Cor}}$). Here, the resulting minimum value of reliability index is $\beta = 3.21$, what corresponds to the failure probability $P_f \approx 9.04 \times 10^{-4}$ (Table 6). The current study leads to reasonable reliability levels for both convalescence and healing periods compared to the structural studies [14]. In addition,

the developed algorithm also identifies the multiple failure modes. The resulting system reliability index $\beta = 5.10$ corresponds to a very small probability of failure $P_f \approx 1.70 \times 10^{-7}$.

For future work, from the accuracy improvement point of view, it is very important to deal with realistic models of geometry, material properties and boundary conditions. At the geometry improvement levels, there are many sophisticated methods for computational representation of bone geometry including medical image software to develop patient-specific models based on CT or MRI data [8]. Additionally, 3D laser scanning of a human mandible may produce accurate surface geometry that can be converted to a solid. At the material property levels, if a method of modulus distribution based on bone density, such as one that can be done with CT/MR techniques, some regions of the bone have a lower level of Young's modulus and thus a different yield limit. Failure would be easier to predict with such technique. At the boundary condition levels, many oblique forces and dynamic studies should be considered in order to predict realistic simulations [26]–[29]. The realistic model can be obtained only when considering dynamic studies (transient analysis). To perform this kind of study, many data about the muscle and applied forces should be measured at several instances (moments). In the current static study, the different forces are represented by 20 input parameters. This number of parameters should be multiplied by the number of instances in dynamic cases. In this case not only a big number of force data is required, but the optimization process and the reliability analysis would be very complicated because of a big number of variables and may also lead to a weak convergence stability. So, a development of an efficient optimization and reliability tools should be performed in order to deal with the big force data.

From the point of view of uncertainty developments, to apply the uncertainty on these future accuracy developments, a very big number of random variables should be taken into consideration that may lead to a very high computing time and a weak convergence stability. In addition, the integration of reliability-based design optimization that defines the best compromise between the healing period minimization, reliability level maximization, leads to new reliability-based design configurations of the mini-plates and screws distribution. Finally, when combining the numerical and experimental studies, it could be possible to determine the target contact pressure value between both fracture surfaces in order to reduce the pain during the bite process.

5. Conclusion

The integration of reliability concepts into mini-plate fixation strategy is considered a novel aspect in this work. A clinical case of a fractured mandible is considered to evaluate the reliability level in both convalescence and healing periods. In the simplified model, the bite force and the associated muscle forces are considered uncertain parameters. According to the clinical observations, there were no complications after the surgical operation and the healing period lasted for about three months. According to the numerical results, the reliability evaluation leads to reasonable values in both convalescence and healing periods.

Compliance with ethical standards

The authors declare that they have no conflict of interest.

Ethical standards

All procedures performed in studies involving human participants were in accordance with the ethical standards of the institutional and/or national research committee and with the 1964 Helsinki declaration and its later amendments or comparable ethical standards.

Human and animal rights statement

This article does not contain any studies with human participants performed by any of the authors but only using panoramic X-ray as a reference for the study.

References

[1] CHAMPY M., LODDE J., SCHMITT R., JAEGER J., MUSTER D., *Mandibular osteosynthesis by miniature screwed plates via a buccal approach*, Journal of Maxillofacial Surgery, 1978, 6, 14–21.

[2] CLAES L., ECKERT-HÜBNER K., AUGAT P., *The fracture gap size influences the local vascularization and tissue differentiation in callus healing Langenbeck's*, Archives of Surgery, 2003, 388, 316–322.

[3] COX T., KOHN M.W., IMPELLUSO T., *Computerized analysis of resorbable polymer plates and screws for the rigid fixation of mandibular angle fractures*, Journal of Oral and Maxillofacial Surgery, 2003, 61, 481–487.

[4] DITLEVSEN O., MADSEN H.O., *Structural reliability methods*, Internet edition, Version 2.2.2, 2005.

[5] DOBLARÉ M., GARCIA J., GÓMEZ M., *Modelling bone tissue fracture and healing*: a review, Engineering Fracture Mechanics, Elsevier, 2004, 71, 1809–1840.

[6] ELLIS E., THROCKMORTON G.S., *Bite forces after open or closed treatment of mandibular condylar process fractures*, Journal of Oral and Maxillofacial Surgery, 2001, 59, 389–395.

[7] ERKMEN E., ŞIMŞEK B., YÜCEL E., KURT A., *Three-dimensional finite element analysis used to compare methods of fixation after sagittal split ramus osteotomy: setback surgery-posterior loading*, British Journal of Oral and Maxillofacial Surgery, 2005, 43, 97–104.

[8] FÅGELBERG E., GRASSI L., ASPENBERG P., ISAKSSON H., *Surgical widening of a stress fracture decreases local strains sufficiently to enable healing in a computational model*, International Biomechanics, 2015, 2, 12–21.

[9] GROSS S., ABEL E., *A finite element analysis of hollow stemmed hip prostheses as a means of reducing stress shielding of the femur*, Journal of Biomechanics, 2001, 34, 995–1003.

[10] HAOFER A., LIND N., *An exact and invariant first-order reliability format*, J. Eng. Mech. ASCE, 1974, 100, 111–121.

[11] KEAVENY T.M., MORGAN E.F., NIEBUR G.L., YEH O.C., *Biomechanics of trabecular bone Annual review of biomedical engineering*, Annual Reviews of Biomedical Engineering, 2001, 3, 307–333.

[12] KELLER T.S., *Predicting the compressive mechanical behavior of bone*, Journal of Biomechanics, 1994, 27, 1159–1168.

[13] KHARMANDA G., *Reliability analysis for cementless hip prosthesis using a new optimized formulation of yield stress against elasticity modulus relationship*, Materials and Design, 2015, 65, 496–504.

[14] KHARMANDA G., EL-HAMI A., SOUZA DE CURSI., *Reliability--Based Design Optimization*, [in:] P. Breitkopt, R.F. Coelho (Eds.), *Multidisciplinary Design Optimization in Computational Mechanics*, Chapter 11: Wiley & Sons, April 2010, ISBN: 9781848211384, Hardback 576 pp.

[15] KHARMANDA M.G., KHARMA M.Y., RISTINMAA M., WALLIN M., *Structural optimization of mini-plates in fixation of human mandible fractures*, NSCM-27, A. Eriksson, A. Kulachenko, M. Mihaescu and G. Tibert (Eds.), KTH, Stockholm, Sweden, October 22–24, 2014.

[16] KOEKENBERG L.J., *Vascularization in the healing of fractures*, Acad. Thesis, Amsterdam, 1963.

[17] KORKMAZ H.H., *Evaluation of different miniplates in fixation of fractured human mandible with the finite element method Oral Surgery*, Oral Medicine, Oral Pathology, Oral Radiology, and Endodontology, 2007, 103, e1–e13.

[18] KROMKA M., MILEWSKI G., *Experimental and numerical approach to chosen types of mandibular fractures cured by means of miniplate osteosynthesis*, Acta of Bioengineering and Biomechanics, 2007, 9, 49.

[19] KROMKA-SZYDEK M., JĘDRUSIK-PAWŁOWSKA M., MILEWSKI G., LEKSTON Z., CIEŚLIK T., DRUGACZ J., VOL B., *Numerical analysis of displacements of mandible bone parts using various elements for fixation of subcondylar fractures*, Acta Bioeng. Biomech., 2010, 12, 11–18.

[20] KUMAR S.T., SARAF S., DEVI S.P., *Evaluation of bite force after open reduction and internal fixation using microplates*, Journal of dentistry, Tehran University of Medical Sciences, 2013, 10, 466.

[21] MESNARD M., *Elaboration et validation d'un protocole de caractérisation de l'articulation temporo-mandibulaire*, Bordeaux University, IST Press, 2005.

[22] RAMOS A., MARQUES H., MESNARD M., *The effect of mechanical properties of bone in the mandible, a numerical case study*, Advnces of Biomechnics and Applications, 2014, 1, 67–76.

[23] REINA-ROMO E., SAMPIETRO-FUENTES A., GÓMEZ-BENITO M., DOMINGUEZ J., DOBLARÉ M., GARCIA-AZNAR J., *Biomechanical response of a mandible in a patient affected with hemifacial microsomia before and after distraction osteogenesis*, Medical Engineering and Physics, 2010, 32, 860–866.

[24] REITZIK M., LEYDEN W.S., *Bone repair in the mandible: a histologic and biometric comparison between rigid and semirigid fixation*, Journal of Oral and Maxillofacial Surgery, 1983, 41, 215–218.

[25] ROTH F.S., KOKOSKA M.S., AWWAD E.E., MARTIN D.S., OLSON G.T., HOLLIER L.H., HOLLENBEAK C.S., *The identification of mandible fractures by helical computed tomography and panorex tomography*, The Journal of Craniofacial Surgery, 2005, 16 (3).

[26] SALLES C., TARREGA A., MIELLE P., MARATRAY J., GORRIA P., LIABOEUF J., LIODENOT J.-J., *Development of a chewing simulator for food breakdown and the analysis of in vitro flavor compound release in a mouth environment*, Journal of Food Engineering, 2007, 82, 189–198.

[27] WALTIMO A., KÖNÖNEN M., *A novel bite force recorder and maximal isometric bite force values for healthy young adults*, European Journal of Oral Sciences, Wiley Online Library, 1993, 101, 171–175.

[28] WODA A., MISHELLANY-DUTOUR A., BATIER L., FRANÇOIS O., MEUNIER J., REYNAUD B., ALRIC M., PEYRON M., *Development and validation of a mastication simulator*, Journal of Biomechanics, 2010, 43, 1667–1673.

[29] ŻMUDZKI J., CHLADEK G., KASPERSKI J., DOBRZAŃSKI L.A., *One versus two implant-retained dentures: comparing biomechanics under oblique mastication forces*, Journal of Biomechanical Engineering, American Society of Mechanical Engineers, 2013, 135, 054503.